Inorg. Chem. **2006**, *45*, 3287–3294

Novel 3D, 2D, and 0D First-Row Coordination Compounds with 4,4′-Bipyridine-*N*,*N*′-dioxide Incorporating Sulfur-Containing Anions

Déborah González Mantero, Antonia Neels,* and Helen Stoeckli-Evans

Institut de Chimie, Université de Neuchâtel, Av. de Bellevaux 51, CH-2007 Neuchâtel, Switzerland

Received November 9, 2005

The reaction of $M(S_2O_6)$ (M = Cu^{II}, Ni^{II}, and Co^{II}) with 4,4′-bipyridine-*N*,*N*′-dioxide (bpdo) results in the formation of novel 3D, 2D, and mononuclear complexes. Complex **1**, $\{[Cu(H_2O)(bpdo)_2](S_2O_6)(H_2O)\}_n$, is a 2-D wavelike polymer with the Cu^{II} ion located on a 2-fold axis and having a distorted square-pyramidal coordination sphere. With Co^{II} and Ni^{II}, 3-D complexes, $\{[M(bpdo)_3](S_2O_6)(C_2H_5OH)_7\}_n$ [M = Co^{II} (**2**), Ni^{II} (**3**)], were obtained. The metal atoms are situated on centers of symmetry and have octahedral environments coordinated to six bpdo molecules. The same reaction in aqueous solution with a metal/ligand ratio of 1:1 results in the formation of mononuclear complexes, $\{[M(bpdo)(H_2O)_5](SO_4)(H_2O)_2\}$ [M = Co^{II} (**4**), Ni^{II} (**5**)], accompanied by the decomposition of the dithionate anions $S_2O_6^{2-}$ to sulfate anions SO_4^{2-}.

Introduction

In the past decade, considerable progress has been made in the design and engineering of multidimensional metal−organic compounds[1] with regard to their potential application in various areas. Extensive studies are related to the porosity of a large variety of materials,[2] and their electronic, magnetic, and optical properties[3] are being exploited. The assembly of metal ions and different multifunctional ligands results in a variety of structures with fascinating architectures, which are potentially useful in solving highly actual problems such as energy and environmental issues.[4]

The prediction of crystal structures is still a difficult task, but their retrospective analysis provides important information for the design of materials with specific properties. For example, to achieve extended multidimensional arrays, metal ions having specific coordination behaviors are combined with functionalized ligand molecules.[2b] The final supramolecular architecture is also influenced by the reaction conditions, the anions, and the solvent used. The influence of counterions and solvent molecules can be drastic because they can exhibit coordinating properties or, in a template role, are involved in noncovalent interactions such as H bonding or $\pi-\pi$ stacking, so stabilizing the metal−organic assembly.

Exo-bidentate ligands such as pyrazine or 4,4′-bipyridine have been widely used and exploited as building blocks in multidimensional polymers.[5] They are linear spacer molecules, but the coordination behavior of the metal and the metal/ligand ratio used is crucial. Recently, it has been shown that 4,4′-bipyridine-*N*,*N*′-dioxide (bpdo), the *N*-oxide of 4,4′-bipyridine, is also very interesting for the construction of multidimensional arrays. bpdo is an O donor ligand, which explains its high affinity to various lanthanide cations.[6] Three-dimensional (3D) networks can be obtained based on the high coordination numbers of the metals involved (≥7).[7] With first-row transition metals, mainly one-dimensional

* To whom correspondence should be addressed. E-mail: antonia.neels@unine.ch. Tel.: +41-32-7182426. Fax: +41-32-7182511.

(1) (a) Desiraju, G. R. *J. Mol. Struct.* **2003**, *656*, 5. (b) Kitagawa, S.; Noro, S. *Comput. Coord. Chem. II* **2004**, *7*, 231. (c) James, S. L. *Chem. Soc. Rev.* **2003**, *32*, 276. (d) Blake, A. J.; Champness, N. R.; Hubberstey, P.; Li, W.-S.; Withersby, M. A.; Schröder, M. *Coord. Chem. Rev.* **1999**, *183*, 117.

(2) (a) Kitagawa, S.; Kitaura, R.; Noro, S. *Angew. Chem., Int. Ed.* **2004**, *43*, 2334. (b) Moulton, B.; Zaworotko, J. *Chem. Rev.* **2001**, *101*, 1629. (c) Rowsell, J. L. C.; Yaghi, O. M. *Microporous Mesoporous Mater.* **2004**, *73*, 3. (d) Kitagawa, S.; Uemura, K. *Chem. Soc. Rev.* **2005**, *34*, 109. (e) Yaghi, O. M.; Li, H.; Groy, T. L. *Inorg. Chem.* **1997**, *36*, 4292. (f) Min, K. S.; Suh, M. P. *Chem.—Eur. J.* **2001**, *7*, 303.

(3) (a) Matsuda, R.; Kitaura1, R.; Kitagawa, S.; Kubota, Y.; Belosludov, R. V.; Kobayashi, T. C.; Sakamoto, H.; Chiba, T.; Takata, M.; Kawazoe, Y.; Mita, Y. *Nature* **2005**, *436*, 238. (b) Eddaoudi, M.; Kim, J.; Rosi, N.; Vodak, D.; Wachter, J.; O'Keeffe, M.; Yaghi, O. M. *Science* **2002**, *295*, 469.

(4) (a) Rosseinsky, M. J. *Microporous Mesoporous Mater.* **2004**, *73*, 15. (b) Jung, O.-S.; Kim, Y. J.; Lee, Y.-A.; Park, J. K.; Chae, H. K. *J. Am. Chem. Soc.* **2000**, *122*, 9921. (c) Chandler, B. D.; Coté, A. P.; Cramb, D. T.; Hill, J. M.; Shimizu, G. K. H. *Chem. Commun.* **2002**, 1900. (d) Ghosh, A. K.; Ghoshal, D.; Zangrando, E.; Ribas, J.; Chaudhuri, N. R. *Inorg. Chem.* **2005**, *44*, 1786.

(5) Roesky, H. W.; Andruh, M. *Coord. Chem. Rev.* **2003**, *236*, 91.

(6) (a) Ma, S.-L.; Qi, C.-M.; Guo, Q.-L.; Zhao, M.-X. *J. Mol. Struct.* **2005**, *738*, 99. (b) Hill, R. J.; Long, D.-L.; Turvey, M. S.; Blake, A. J.; Champness, N. R.; Hubberstey, P.; Wilson, C.; Schroeder, M. *Chem. Commun.* **2004**, 1792. (c) Zhu, W. X.; He, Y. *Coord. Chem.* **2002**, *55*, 251. (d) Seward, C.; Wang, S. *Can. J. Chem.* **2001**, *79*, 1187. (e) Agarwal, R. K.; Agarwal, H. *J. Saudi Chem. Soc.* **2000**, *4*, 251. (f) Long, D.-L.; Blake, A. J.; Champness, N. R.; Wilson, C.; Schroeder, M. *J. Am. Chem. Soc.* **2001**, *123*, 3401.

10.1021/ic051934x CCC: $33.50
Published on Web 03/18/2006

Chart 1. Possible Coordination Modes for bpdo

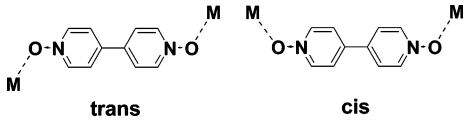

Chart 2. Possible Participation of bpdo in H Bonding

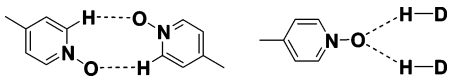

(1D) coordination polymers have been obtained.[8] Only a few examples exist for *homoleptic* higher dimensional polymers.[9] The relatively low space-demanding nature of the pyridyl-*N*-oxide donor group, combined with the orientation of the lone pairs on the pyridyl-*N*-oxide O atoms, results in a relatively high flexibility regarding its coordination behavior. If bpdo coordinates in a bridging mode, two different coordination geometries are found (trans and cis; Chart 1).

For a perfect cis coordination mode, the torsion angle M−O−O−M should be 0°. To the best of our knowledge, this has not been observed to date. A search in the Cambridge Crystallographic Database (CCSD)[10] shows that the trans form dominates but the distribution about the maximum, at ca. 50°, shows a relatively high number of structures adopting the cis conformation (Figure 1S in the Supporting Information).

The coordination flexibility of bpdo can also be demonstrated by the large variation in the value of the M−O−N angle. This value ranges from 105° to 150°, with a maximum at 125°, especially for first-row transition-metal complexes (Figure 2S in the Supporting Information). Besides being a strongly coordinating ligand, bpdo is a very good H-bond acceptor. This has been shown by its use in the construction of a number of multidimensional H-bonded polymers (Chart 2).[11]

We observed, in addition, that the neighboring C−H function in the aromatic ring can lead to the formation of H bonds between the coordinated bpdo molecules, resulting in a stabilization of the metal coordination polyhedron (Chart 3).

Chart 3. Chelating Properties of bpdo Involving a C−H H-Donor Function

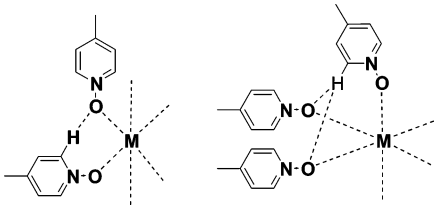

Here we describe the construction of 3D, 2D, and 0D metal−organic compounds using first-row transition metals in combination with bpdo. The reactions of Cu^{II}, Co^{II}, and Ni^{II} with bpdo in the ratios 1:1, 1:2, and 1:3, respectively, were studied. Because of the different coordination behaviors of the metals, 1:1 and 1:3 complexes were formed with Co^{II} and Ni^{II}, while the 1:2 complex was formed with Cu^{II}. New structure types have been observed mainly because of the use of $S_2O_6^{2-}$ as a counterion. A search in the CCSD revealed the presence of over a hundred crystal structures containing the dithionate anion. Interestingly, in only about 10% of the structures is the anion coordinated to the metal, and in only 5% is the dithionate anion acting as a bridging ligand in some polymeric complexes.[12] More often than not, the space-demanding anion acts through its O atoms as an H-bond acceptor and as such it is a useful network builder. In the majority of the published structures, the H bonds are formed with NH or OH functions of the cationic complex fragment. In the absence of these functions, solvent molecules are cocrystallized to establish strong solvent−anion interactions.[13] This has been observed for the 2D complex **1**, where coordinated and uncoordinated water molecules are present in the structure. Anionic dithionate−water chains are formed in the channels between the cationic $\{[Cu(bpdo)_2(H_2O)]^{2+}\}_n$ wavelike sheets. Keeping the compound under atmospheric conditions results in an uncontrolled decomposition due to the loss of water. bpdo is also able to participate through its aromatic C−H functions in intermolecular interactions with the dithionate anions, and this has been observed for complexes **2** and **3**. The cationic $\{M(bpdo)_3]^{2+}\}_n$ framework possesses pores filled by the dithionate anions and initially by ethanol molecules of crystallization. When these compounds are exposed to air, the ethanol molecules are replaced

(7) (a) Long, D.-L.; Hill, R. J.; Blake, A. J.; Champness, N. R.; Hubberstey, P.; Proserpio, D. M.; Wilson, C.; Schroeder, M. *Angew. Chem., Int. Ed.* **2004**, *43*, 1851. (b) Long, D.-L.; Blake, A. J.; Champness, N. R.; Wilson, C.; Schroeder, M. *Angew. Chem., Int. Ed.* **2001**, *40*, 2444. (c) Ma, S.-L.; Zhu, W.-X.; Huang, G.-H.; Yuan, D.-Q.; Yan, X. *J. Mol. Struct.* **2003**, *646*, 89. (d) Long, D.-L.; Blake, A. J.; Champness, N. R.; Wilson, C.; Schroeder, M. *Chem.—Eur. J.* **2002**, *8*, 2026.

(8) (a) Tian, J.-L.; Yan, S.-P.; Liao, D.-Z.; Jiang, Z.-H.; Cheng, P. *Inorg. Chem. Commun.* **2003**, *6*, 1025. (b) Nedelcu, A.; Zak, Z.; Madalan, A. M.; Pinkas, J.; Andruh, M. *Polyhedron* **2003**, *22*, 789. (c) Seidel, S. R.; Tabellion, F. M.; Arif, A. M.; Stang, P. J. *Isr. J. Chem.* **2001**, *41*, 149. (d) Plater, M. J.; Foreman, M. R.; Slawin, A. M. Z. *Inorg. Chim. Acta* **2000**, *303*, 132. (e) Yadava, C. L.; Tripathi, S.; Ahuja, I. S. *Trans. Met. Chem.* **1986**, *11*, 295.

(9) (a) Long, D.-L.; Hill, R. J.; Blake, A. J.; Champness, N. R.; Hubberstey, P.; Wilson, C.; Schroeder, M. *Chem.—Eur. J.* **2005**, *11*, 1384. (b) Ma, B.-Q.; Sun, H.-L.; Gao, S.; Xu, G.-X. *Inorg. Chem.* **2001**, *40*, 6247.

(10) Allen, F. H. *Acta Crystallogr.* **2002**, *B58*, 380.

(11) (a) Ma, B.-Q.; Sun, H.-L.; Gao, S. *Inorg. Chem.* **2005**, *44*, 837. (b) Ma, B.-Q.; Sun, H.-L.; Gao, S. *Chem. Commun.* **2003**, 2164. (c) Ma, B.-Q.; Gao, S.; Sun, H.-L.; Xu, G.-X. *J. Chem. Soc., Dalton Trans.* **2001**, *2*, 130. (d) Blake, A. J.; Brett, M. T.; Champness, N. R.; Khlobystov, A. N.; Long, D.-L.; Wilson, C.; Schroeder, M. *Chem. Commun.* **2001**, *21*, 2258.

(12) (a) Bernhardt, P. V.; Dyahningtyas, T. E.; Han, S. C.; Harrowfield, J. M.; Kim, I. C.; Kim, Y.; Koutsantonis, G. A.; Rukmini, E.; Thuery, P. *Polyhedron* **2004**, *23*, 869. (b) Kim, Y.; Skelton, B. W.; White, A. H. *Acta Crystallogr., Sect. C: Cryst. Struct. Commun*. **2003**, *59*, m546. (c) Neels, A.; Alfonso, M.; Mantero, D. G.; Stoeckli-Evans, H. *Chimia* **2003**, *57*, 619. (d) Bernhardt, P. V.; Hambley, T. W.; Lawrance, G. A. *Aust. J. Chem.* **1990**, *43*, 699. (e) Donlevy, T. M.; Gahan, L. R.; Hambley, T. W.; Hanson, G. R.; Markiewicz, A.; Murray, K. S.; Swann, I. L.; Pickering, S. R. *Aust. J. Chem.* **1990**, *43*, 1407. (f) Rusanov, E. B.; Ponomarova, V. V.; Komarchuk, V. V.; Stoeckli-Evans, H.; Fernandez-Ibanez, E.; Stoeckli, F.; Sieler, J.; Domasevitch, K. V. *Angew. Chem., Int. Ed.* **2003**, *42*, 2499. (g) Corbin, K. M.; Glerup, J.; Hodgson, D. J.; Lynn, M. H.; Michelsen, K.; Nielsen, K. M. *Inorg. Chem.* **1993**, *32*, 18. (h) Platt, A. W. G.; Fawcett, J.; Hughes, R. S.; Russell, D. R. *Inorg. Chim. Acta* **1999**, *295*, 146. (i) Fawcett, J.; Platt, A. W. G.; Russell, D. R. *Inorg. Chim. Acta* **1998**, *274*, 177.

(13) (a) Keene, F. R.; Snow, M. R.; Stephenson, P. J.; Tiekink, E. R. T. *Inorg. Chem.* **1988**, *27*, 2040. (b) Towle, D. K.; Botsford, C. A.; Hodgson, D. J. *Inorg. Chim. Acta* **1988**, *141*, 167. (c) Buchen, T.; Hazell, A.; Jessen, L.; McKenzie, C. J.; Nielsen, L. P.; Pedersen, J. Z.; Schollmeyer, D. *J. Chem. Soc., Dalton Trans.* **1997**, 2697. (d) Tong, M.-L.; Zheng, S.-L.; Chen, X.-M. *Chem.—Eur. J.* **2000**, *6*, 3729.

Table 1. Crystal and Structure Refinement Data for **1**−**5**

	1	**2**	**3**	**4**	**5**
formula	$C_{20}H_{20}N_4O_{12}S_2Cu$	$C_{44}H_{66}N_6O_{19}S_2Co$	$C_{44}H_{66}N_6O_{19}S_2Ni$	$C_{10}H_{22}N_2O_{13}SCo$	$C_{10}H_{22}N_2O_{13}SNi$
fw	636.06	1106.08	1105.86	469.29	469.07
λ (Å)	0.710 73	0.710 73	0.710 73	0.710 73	0.710 73
T (K)	173	253	253	253	253
cryst syst	monoclinic	monoclinic	monoclinic	monoclinic	monoclinic
space group	$P2/n$	$C2/c$	$C2/c$	$P2_1/n$	$P2_1/n$
a (Å)	9.7716(9)	20.681(4)	20.828(5)	7.137(1)	7.1380(8)
b (Å)	9.8378(7)	14.135(2)	13.499(4)	25.432(2)	25.244(3)
c (Å)	11.9907(12)	19.564(4)	20.020(5)	10.226(1)	10.211(1)
β (deg)	90.770(8)	107.48(2)	106.18(2)	92.59(1)	92.173(9)
V (Å^3)	1152.6(2)	5455(2)	5406(2)	1854.2(3)	1838.5(4)
Z	2	4	4	4	4
ρ_{calcd} (Mg m^{-3})	1.833	1.347	1.359	1.681	1.695
μ (mm^{-1})	1.207	0.466	0.512	1.107	1.238
reflns collected	12302	16114	16636	19638	12264
indep reflns	2180	5167	4826	3313	3475
indep reflns >2σ(I)	1995	2390	1027	2812	2946
no. of param	186	232	102	274	274
R1[a] [$I > 2\sigma(I)$]	0.027	0.056	0.150	0.033	0.031
wR2[b] [$I > 2\sigma(I)$]	0.066	0.120	0.314	0.078	0.086
S	1.071	0.770	0.765	1.025	1.042
$\Delta\rho_{max}/\Delta\rho_{min}$ (e Å^{-3})	0.349/−0.450	0.428/−0.441	1.323/−0.533	0.760/−0.309	0.978/−0.559

[a] $R1 = \sum||F_o| - |F_c||/\sum|F_o|$. [b] $wR2 = [\sum w(F_o^2 - F_c^2)^2/\sum wF_o^4]^{1/2}$.

by water molecules over a period of time. This results in the destruction of the overall structure, which has been verified by X-ray powder diffraction (XRPD). This is probably due to the important changes in the intermolecular interactions involving the solvent molecules of crystallization.

It will be shown that the architecture of the synthesized complexes is influenced not only by the template effect and the formation of extensive H bonds involving the complex cations and the dithionate anions $S_2O_6^{2-}$ but also by the use of different solvents and metal/ligand ratios.

Experimental Section

Materials. All chemicals were of analytical grade and were used as received without further purification. Metal dithionates were synthesized by the Inorganic Chemistry Department of the University of Kiev.

Physical Measurements. IR spectra were recorded with a Perkin-Elmer Spectrum One spectrometer in transmission mode, and spectra were collected as KBr pellets. The elemental microanalyses were performed by the Microanalysis Service of the Laboratory of Pharmaceutical and Organic Propedeutical Chemistry at the University of Geneva (Geneva, Switzerland). Thermogravimetric (TG) analyses were carried out using a Mettler 4000 module. Samples were introduced in a closed aluminum oxide crucible and heated at a rate of 5 °C min^{-1} under nitrogen at atmospheric pressure.

Synthesis of 1. A solution of $CuS_2O_6{\cdot}6H_2O$ (0.5 mmol, 0.166 g) dissolved in 5 mL of ethanol was added to a solution of bpdo (1 mmol, 0.188 g) dissolved in 5 mL of ethanol. A red precipitate was formed immediately. This precipitate dissolves slowly, and upon slow evaporation of the solvent, green blocklike crystals were obtained. **1** is unstable and hygroscopic. Consequently, no elemental analysis was carried out. IR (cm^{-1}): 3421 (br, m), 3127 (br, s), 1644 (m), 1594 (m), 1511 (w), 1470 (w), 1400 (s), 1214 (m), 1182 (m), 1118 (w), 987 (w), 858 (w), 846 (w), 795 (w), 729 (w), 607 (w), 567 (w), 508 (w), 496 (w).

Synthesis of 2. An ethanolic solution (10 mL) of $CoS_2O_6{\cdot}6H_2O$ (0.5 mmol, 0.163 g) was gently added to an ethanolic solution (10 mL) of bpdo (1 mmol, 0.188 g). After 1 day, orange blocklike crystals were obtained. Elem anal. Calcd for $C_{30}H_{36}CoN_6O_{18}S_2$: C, 40.41; H, 4.07; N, 9.42. Found: C, 40.84; H, 3.69; N, 9.27. IR (cm^{-1}): 3114 (br, s), 2418 (w), 1621 (br, w), 1546 (w), 1471 (s), 1401 (s), 1322 (w), 1224 (s), 1180 (s), 1029 (m), 984 (m), 837 (m), 700 (w), 553 (m), 511 (w).

Synthesis of 3. An ethanolic solution (10 mL) of $NiS_2O_6{\cdot}6H_2O$ (0.5 mmol, 0.163 g) was gently added to an ethanolic solution (10 mL) of bpdo (1 mmol, 0.188 g). After 1 day, orange needlelike crystals were obtained. Elem anal. Calcd for $C_{30}H_{36}NiN_6O_{18}S_2$: C, 40.42; H, 4.07; N, 9.43. Found: C, 40.46; H, 3.91; N, 9.23. IR (cm^{-1}): 3116 (br, s), 1621 (br, w), 1546 (w), 1470 (s), 1401 (s), 1322 (w), 1222 (s), 1177 (s), 1028 (m), 984 (m), 836 (m), 700 (w), 552 (m), 475 (w).

Synthesis of 4. An ethanolic solution (10 mL) of bpdo (1 mmol, 0.188 g) was gently added to an aqueous solution (10 mL) of $CoS_2O_6{\cdot}6H_2O$ (0.5 mmol, 0.163 g). Upon slow evaporation, orange needlelike crystals were obtained. This compound can also be obtained directly using $CoSO_4$ instead of the corresponding dithionate salt following the same procedure. Elem anal. Calcd for $C_{10}H_{22}CoN_2O_{13}S$: C, 25.59; H, 4.73; N, 5.97. Found: C, 24.6; H, 4.29; N, 5.48. IR (cm^{-1}): 3132 (br, s), 1636 (br, w), 1550 (w), 1474 (m), 1400 (s), 1326 (w), 1237 (m), 1185 (m), 1090 (w), 1031 (w), 986 (w), 839 (m), 699 (w), 559 (w), 520 (w), 485 (w).

Synthesis of 5. An ethanolic solution (10 mL) of bpdo (1 mmol, 0.188 g) was gently added to an aqueous solution (10 mL) of $NiS_2O_6{\cdot}6H_2O$ (0.5 mmol, 0.163 g). Upon slow evaporation, green needlelike crystals were obtained. This compound can also be obtained directly using $NiSO_4$ instead of the corresponding dithionate salt, following the same procedure. Elem anal. Calcd for $C_{10}H_{22}NiN_2O_{13}S$: C, 25.61; H, 4.73; N, 5.97. Found: C, 25.12; H, 4.63; N, 5.80. IR (cm^{-1}): 3128 (br, s), 1650 (br, w), 1548 (w), 1475 (m), 1400 (s), 1324 (w), 1242 (w), 1188 (w), 1115 (m), 1030 (w), 982 (w), 840 (w), 763 (w), 698 (w), 622 (w), 559 (w), 506 (w), 489 (w).

Crystallographic Analyses. Crystallographic details for complexes **1**−**5** are given in Table 1, and significant bond lengths and bond angles are listed in Tables 2 and 4. Additional crystallographic information has been placed in the Supporting Information.

Scheme 1. Synthesis of New First-Row Transition-Metal Coordination Compounds (**1**−**5**) with bpdo

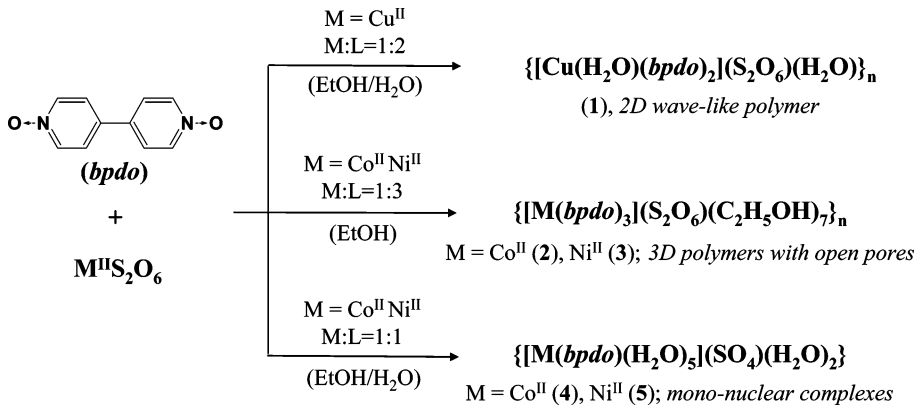

Table 2. Selected Bond Lengths (Å) and Angles (deg) of Complexes **1**−**3**

	Compound **1**[a]		
Cu1−O1	1.918(1)	Cu1−O2	2.004(1)
Cu1−O3	2.262(2)		
O1−Cu1−O2	85.46(6)	O1−Cu1−O2a	93.95(6)
O1−Cu1−O3	92.02(5)	O2−Cu1−O3	98.48(4)
O1−Cu1−O1a	175.96(7)	O2−Cu1−O2a	163.03(6)
	Compound **2**[b]		
Co1−O1	2.065(3)	Co1−O3	2.073(2)
Co1−O2	2.088(3)		
O1−Co1−O2	91.8(1)	O1−Co1−O3a	88.2(1)
O1−Co1−O3	91.8(1)	O2−Co1−O3	94.8(1)
O1−Co1−O1a	180	O2−Co1−O3a	85.2(1)
O1−Co1−O2a	88.2(1)		
	Compound **3**[b]		
Ni1−O1	2.107(14)	Ni1−O3	2.009(13)
Ni1−O2	2.038(11)		
O1−Ni1−O2	91.6(5)	O1−Ni1−O3a	87.8(5)
O1−Ni1−O3	92.2(5)	O2−Ni1−O3	94.9(5)
O1−Ni1−O1a	180	O2−Ni1−O3a	85.1(5)
O1−Ni1−O2a	88.4(5)		

[a] (a) $^1/_2 - x, y, ^1/_2 - z$. [b] (a) $^1/_2 - x, ^1/_2 - y, 1 - z$.

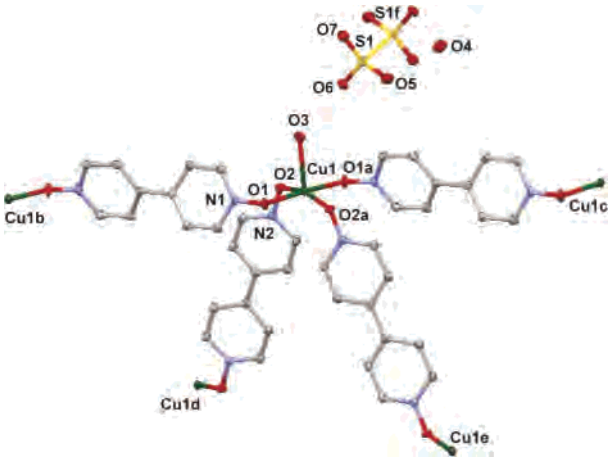

Figure 1. ORTEP[17] figure of **1** (50% probability ellipsoids), with symmetry operations (a) $^1/_2 - x, y, ^1/_2 - z$; (b) $x, y, z + 1$; (c) $x, y, z - 1$; (d) $-x, -y, 1 - z$; (e) $1 - x, -y, -z$; (f) $-x, 2 - y, -z$.

Results and Discussion

Syntheses. Complexes **1**−**5** have been obtained by the reaction of $M(S_2O_6)$ ($M = Cu^{II}$, Co^{II}, Ni^{II}) with bpdo in different solvents (Scheme 1). The metal/ligand ratio and the solvent choice play an important role with regard to the variation in dimensionality of the compounds obtained. The metal/ligand ratios of 1:2 and 1:3 result in homoleptic 2D (**1**) and 3D (**2** and **3**) structures, respectively. The ratio of 1:1 results in the formation of mononuclear complexes (**4** and **5**). Complexes **1**−**3** were crystallized by slow diffusion of the starting materials, $M(S_2O_6)$ and bpdo, each being dissolved in an ethanolic solution. The use of water as the solvent results in the decomposition of the dithionate anions $S_2O_6^{2-}$ into sulfate anions SO_4^{2-}. Complexes **1**−**3** were obtained in an ethanolic solution and present unique and fascinating structures.

Table 3. C−H···O Intramolecular Interactions (Å, deg) for Compounds **2** and **3**[a]

	D−H	H···A	D···A	D−H···A
		Compound **2**		
C10−H10···O3	0.93	2.49	2.951(5)	111
C10−H10···O1a	0.93	2.55	3.269(4)	135
C15−H15···O1	0.93	2.27	3.066(5)	143
		Compound **3**		
C10−H10···O1a	0.93	2.24	3.04(2)	144
C15−H15···O1	0.93	2.26	3.06(3)	143

[a] (a) $^1/_2 - x, ^1/_2 - y, 1 - z$.

Table 4. Selected Bond Lengths (Å) and Angles (deg) of Complexes **4** and **5**

	Compound **4**		
Co1−O1	2.119(2)	Co1−O5	2.072(2)
Co1−O3	2.053(2)	Co1−O6	2.080(2)
Co1−O4	2.092(2)	Co1−O7	2.089(2)
O4−Co1−O7	93.69(8)	O1−Co1−O7	93.21(7)
O5−Co1−O6	90.67(7)	O3−Co1−O4	88.75(8)
O5−Co1−O7	92.80(7)	O3−Co1−O5	178.75(7)
O6−Co1−O7	175.08(7)	O3−Co1−O6	90.54(7)
O1−Co1−O3	87.23(8)	O3−Co1−O7	85.97(7)
O1−Co1−O4	171.74(8)	O4−Co1−O5	91.59(8)
O1−Co1−O5	92.59(8)	O4−Co1−O6	89.70(8)
O1−Co1−O6	83.14(7)		
	Compound **5**		
Ni1−O1	2.081(2)	Ni1−O5	2.048(2)
Ni1−O3	2.040(2)	Ni1−O6	2.043(2)
Ni1−O4	2.056(2)	Ni1−O7	2.045(2)
O4−Ni1−O7	92.85(8)	O1−Ni1−O7	93.91(7)
O5−Ni1−O6	90.38(6)	O3−Ni1−O4	89.44(8)
O5−Ni1−O7	93.18(6)	O3−Ni1−O5	178.63(7)
O6−Ni1−O7	175.16(7)	O3−Ni1−O6	89.54(6)
O1−Ni1−O3	85.54(7)	O3−Ni1−O7	86.82(6)
O1−Ni1−O4	171.35(7)	O4−Ni1−O5	91.93(8)
O1−Ni1−O5	93.09(7)	O4−Ni1−O6	90.30(8)
O1−Ni1−O6	82.63(7)		

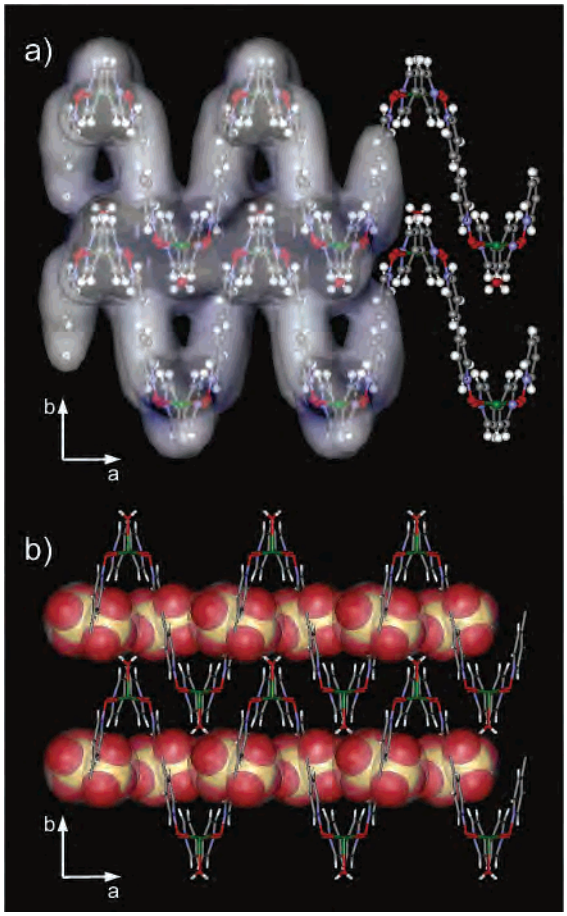

Figure 2. 2D wavelike structure in **1**: (a) $S_2O_6^{2-}$ anions are omitted; (b) H-bonded chains of $S_2O_6^{2-}$ anions and H_2O molecules are shown as a space-filling model.[18]

Crystal Structure of 1. In this 2D network, the Cu^{II} coordination sphere is formed by four bpdo ligands and one water molecule, which occupy equatorial and axial positions, respectively (Figure 1). The Cu^{II} ion is located on a 2-fold rotation axis, and the coordination sphere can be described as distorted square-pyramidal with $\tau = 0.22$ ($\tau = 0$ for perfect square pyramidal and $\tau = 1$ for perfect trigonal bipyramidal).[14] The coordination Cu···O bond distances for the bpdo ligand are comparable with those described in the literature (Table 2).[8b,9b] Cu−O−N bond angles of 119.0(1)° and 119.7(1)° are observed for Cu1−O1−N1 and Cu1−O2−N2, respectively.

The bpdo ligand molecules link adjacent CuO_5 centers into two dimensions, resulting in the formation of a 2D wavelike structure (Figure 2a). bpdo adopts the trans geometry, coordinating to the metal centers with dihedral angles of 175.4(1)° for Cu1−O1−O1b−Cu1b and 180° for Cu1−O2−O2d−Cu1d. This results in intramolecular metal−metal distances of 12.250(1) and 11.991(1) Å, respectively. One bpdo ligand molecule is crystallographically planar, while the other exhibits a dihedral angle of 22.18(5)° between the pyridine-*N*-oxide planes. Cocrystallized water molecules and dithionate anions are connected by H bonds to form negatively charged chains running in square channels (4 × 4 Å), parallel to the crystallographic *ac* diagonal, created by the cationic $\{[Cu(bpdo)_2(H_2O)]^{2+}\}_n$ 2D structure (Figure 2b).

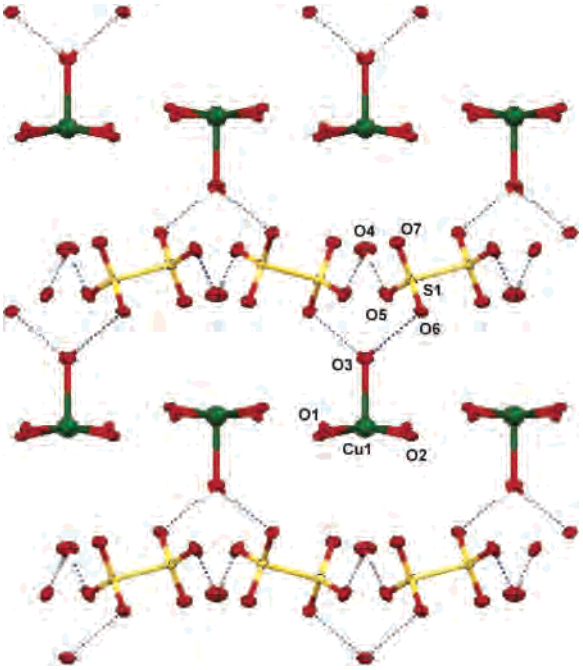

Figure 3. MERCURY[17] plot of **1** showing the 1D H bonding involving the $S_2O_6^{2-}$ anions and the coordinated and uncoordinated water molecules.

The coordinated water molecules are H-bonded to the dithionate anions and hence link the polymer chains to form a 3D structure (Figure 3 and Table 1S in the Supporting Information). The wavelike polymeric sheets are stacked, with the shortest Cu−Cu intermolecular distance being 7.692(1) Å.

Crystal Structures of 2 and 3. Compounds **2** and **3** are isostructural and isomorphous (space group *C*2/*c*). Therefore, only structure **2** will be discussed in detail. Complex **2** is a 3D porous material. The Co^{II} atoms lie on inversion centers and have CoO_6 octahedral coordination environments (Figure 4). Each metal is coordinated to six bpdo molecules, and the Co−O bond distances are comparable with those found in the literature (Table 2).[8b,d,11c,d]

Within the coordination sphere of the Co atom, C−H···O intramolecular interactions between the coordinating bpdo molecules are observed (Chart 3 and Figure 5). As a result, the Co−O bond distances where the N−O oxygen is a H-bond acceptor for a nearby C−H H-donor function are slightly shorter (ca. 0.02 Å) than the other Co−O distances (Table 3).

The bridging nature of the six coordinated bpdo ligands is responsible for the formation of the 3D network. The bpdo ligand molecules show both the trans and the cis coordination modes, with torsion angles of 180° for Co1−O3−O3f−Co1f and 44.8(2)° for Co1−O1−O2e−Co1e (Figure 5). For each Co^{II} ion, two coordinated bpdo ligands have a trans coordination mode and the other four a cis coordination mode. This results in a longer intramolecular metal−metal distance for the trans connection compared to that for the cis connection, 12.525(2) and 12.068(2) Å, respectively. The

(14) Addison, A. W.; Rao, T. N.; Reedijk, J.; van Rijn, J.; Verschoor, G. C. *J. Chem. Soc., Dalton Trans.* **1984**, *7*, 1349.

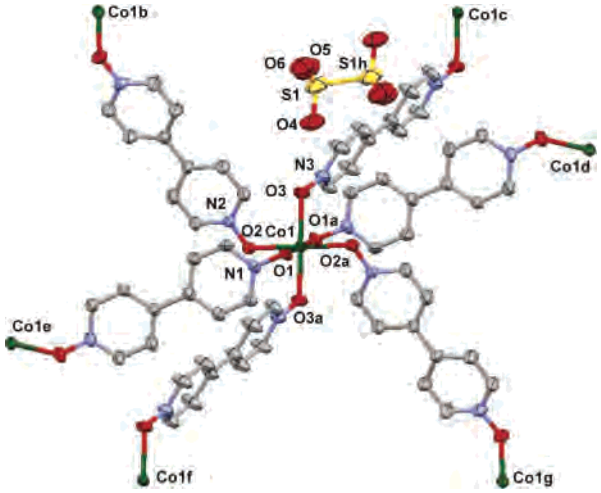

Figure 4. ORTEP[17] figure of **2** (30% probability ellipsoids) with symmetry operations (a) $^1/_2 - x$, $^1/_2 - y$, $1 - z$; (b) $^1/_2 - x$, $^1/_2 - y$, $1.5 - z$; (c) $^1/_2 + x$, $-^1/_2 + y$, z; (d) $^1/_2 - x$, $-^1/_2 + y$, $^1/_2 - z$; (e) $^1/_2 - x$, $^1/_2 + y$, $1.5 - z$; (f) $-^1/_2 + x$, $^1/_2 + y$, z; (g) $^1/_2 - x$, $^1/_2 + y$, $^1/_2 - z$; (h) $^1/_2 - x$, $-^1/_2 - y$, $1 - z$.

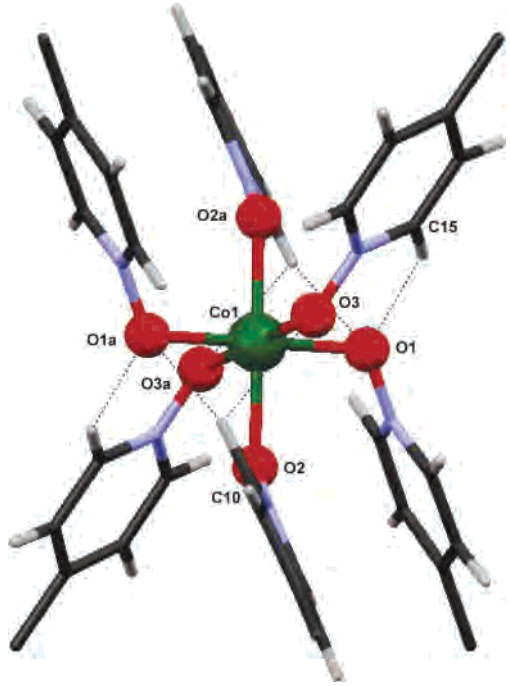

Figure 5. MERCURY[17] plot of **4** showing the stabilizing effect of the intramolecular C−H···O hydrogen bonds.

cis coordination is related to a small deviation from coplanarity of the pyridine-*N*-oxide moieties [8.1(2)°], while the trans-coordinated ligand exhibits crystallographic planarity. The coordination flexibility of bpdo is reflected by the Co−O−N angles, 119.4(2)° and 127.1(2)° for Co1−O1−N1 and Co1−O2−N2, respectively. The 3D coordination polymer has square channels, with dimensions of about 8.3 × 8.5 Å, parallel to the crystallographic *c* axis, and 6.7 × 4.8 Å, parallel to the *b* axis. They are initially filled with ethanol molecules (Figure 6a), and the porosity is estimated to be about 50% for the guest free compound. The recently published structure of $\{[Sc(bpdo)_3](CF_3SO_3)_3(CH_3OH)_{2.7}(H_2O)_3\}_n$[9a] displays the same framework topology but has 35% porosity because of the metal/anion ratio of 1:3

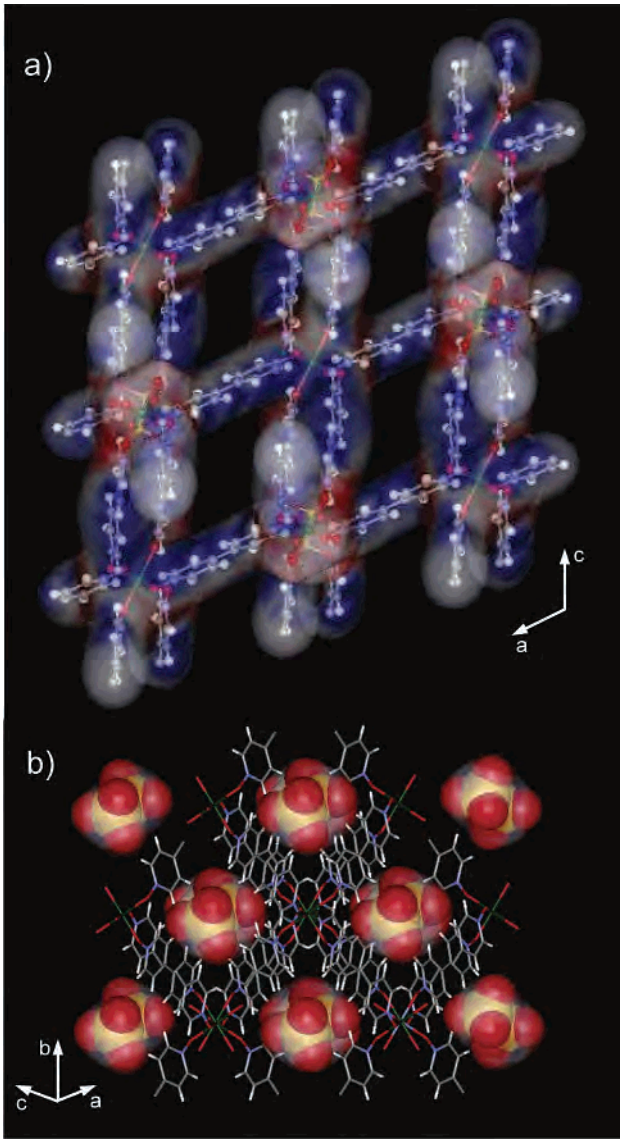

Figure 6. 3D structure in **2**: (a) space-filling model[18] showing open pores; (b) $S_2O_6^{2-}$ anions shown as a space-filling model in the cavities.

compared to 1:1 for **2**. The dithionate anions, fixed by C−H···O interactions to the framework, are located in small square channels (4 × 4 Å) running parallel to the crystallographic *ac* diagonal. This has no influence on the open-channel structure of **2** (Figure 6b). The shortest through-space metal−metal distance is only slightly shorter [11.910(2) Å] than the shortest metal−metal distance mediated through the ligand [12.068(2) Å].

Crystal Structures of 4 and 5. Compounds **4** and **5** are isostructural and isomorphous (space group $P2_1/n$). Therefore, only structure **4** will be discussed in detail. The synthesis of compound **4** was carried out in an aqueous solution, in contrast to the syntheses of compounds **1**−**3**, performed in an ethanolic solution. Under these conditions, the dithionate anions decompose to sulfate anions and sulfur dioxide; hence, sulfate anions are found in the structure of **4**. The presence of water during the synthesis has a direct influence not only on the decomposition of the dithionate anions but also on the loss of dimensionality because the water molecules are involved in the coordination sphere of

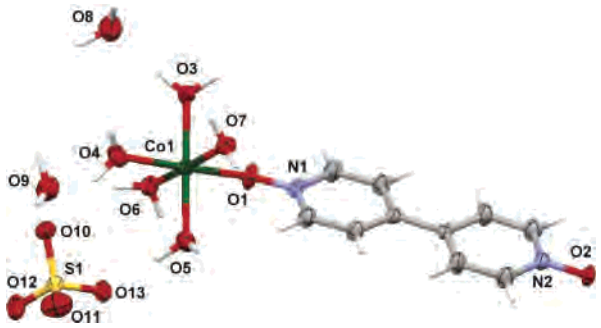

Figure 7. ORTEP[17] figure of **4** (50% probability ellipsoids).

the metal ions. Complex **4** is a mononuclear compound, with the Co^{II} ion in a distorted octahedral coordination environment (Figure 7 and Table 4). The metal is coordinated to one bpdo molecule and five water molecules, resulting in a CoO_6 coordination sphere. The bpdo ligand coordinated to the metal is nearly planar, with a small twist angle of 2.1(1)°. The Co−O−N angle is relatively large [132.3(2)°] compared to the same angles observed in **1**−**3** (average value 121.3°). At the same time, the Co−O(bpdo) bond distance is longer and the bpdo N−O distance is shorter in the mononuclear complex [2.119(2) and 1.317(3) Å, respectively] compared to the same bond distances in the 3D compound **2** [$(Co-N)_{av} = 2.075(3)$ Å and $(N-O)_{av} = 1.334(3)$ Å, respectively]. The remaining $Co-O_{water}$ distances in **4** are very similar, with an average value of 2.077(2) Å, which agrees with the values found for CoO_6 systems in the CCSD [$(Co-O)_{av} = 2.08$ Å for 692 hits].

The mononuclear units are connected via H bonds formed between the coordinated water molecules and the bpdo molecules with the cocrystallized sulfate anions and water molecules. This results in a mutual connection of complex molecules in a head-to-tail manner (Figure 8 and Table 1S in the Supporting Information). Furthermore, adjacent bpdo ligands are involved in weak $\pi-\pi$-stacking interactions (3.57 Å), leading to a ladder-type structure. A similar arrangement was reported earlier for $\{[Fe(bpdo)(H_2O)_5](SO_4)(H_2O)_4\}$.[15]

IR, Thermal Analyses, and XRPD

IR spectra were carried out on powdered samples of complexes **1**−**5** and compared to the spectrum of the free bpdo ligand. A clear shift of the N−O vibration band to lower frequencies was observed for complexes **1**−**3** with values of 1213, 1223, and 1222 cm^{-1}, respectively, compared to 1240 cm^{-1} in the free ligand. This also agrees with the N−O bond distances being much longer in these polymeric complexes, where the N−O distances range from 1.325(4) to 1.348(2) Å, compared to 1.314(3) Å in the structure of the free bpdo ligand.[16] In complexes **4** and **5**, a broad band

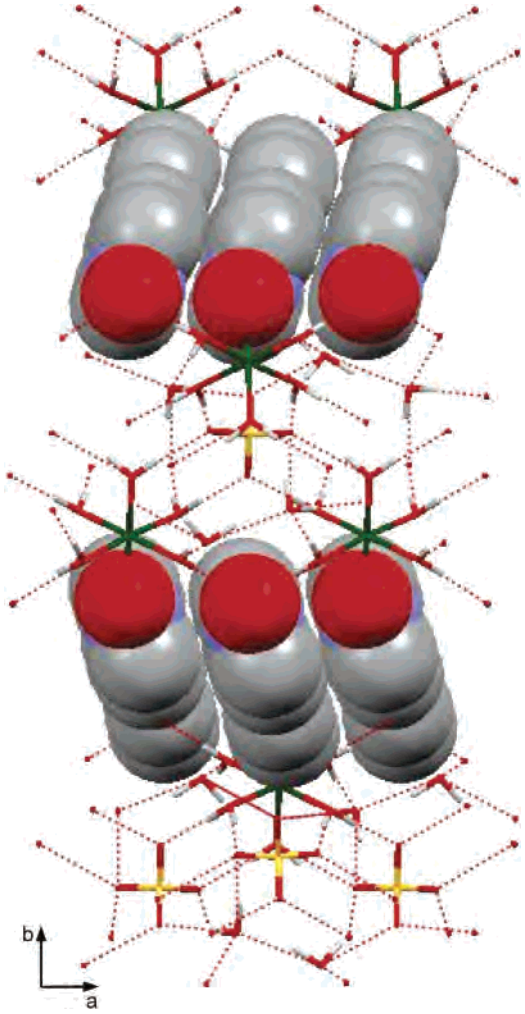

Figure 8. View of the H-bonding system in **4**, showing how it cross-links the $\pi-\pi$-stacked mononuclear complexes (space-filling) to form a 3D network.

is observed around 1237 cm^{-1}, representative for the N−O vibration bands of the coordinated and uncoordinated parts of the bpdo ligand. Accordingly, the N−O distances in the crystal structures of complexes **4** and **5** are only slightly different from the same distances in the free ligand. Interestingly, the N−O distance of the coordinated part remains unchanged, with bond distances of 1.317(3) Å for **4** and 1.318(2) Å for **5**. However, the N−O bond in the part participating only in H bonding increases, being 1.328(3) Å for both **4** and **5**. In all of the spectra of complexes **1**−**5**, a strong band at 1400 cm^{-1} is observed for the S═O vibration in the $S_2O_6^{2-}$ (**1**−**3**) or the SO_4^{2-} (**4** and **5**) anions.

Thermal analyses and XRPD experiments have been carried out for compounds **2**−**5**. No thermal analysis was carried out for compound **1** because of its fast decomposition under atmospheric conditions. Compounds **2** and **3** are 3D metal−organic polymers having ca. 50% of their volumes occupied by molecules of ethanol. Removal of these guest molecules without collapse of the host structure would result in permanent porosity, which is crucial for adsorption studies. The TG curve of compound **2** shows the loss of solvent molecules in two steps until 190 °C. The loss of one bpdo molecule and sulfur dioxide occurs at 300 °C. The TG curve

(15) Ma, B.-Q.; Gao, S.; Sun, H.-L.; Xu, G.-X. *CrystEngComm* **2001**, *35*, 1.
(16) Thaimattam, R.; Reddy, D. S.; Xue, F.; Mak, A. N.; Desiraju, G. R. *J. Chem. Soc., Perkin Trans. 2* **1998**, 1783.
(17) Bruno, I. J.; Cole, J. C.; Edgington, P. R.; Kessler, M. K.; Macrae, C. F.; McCabe, P.; Pearson, J.; Taylor, R. *Acta Crystallogr.* **2002**, *B58*, 389.
(18) WebLab ViewerLite 3.7; Molecular Simulations Inc.: Cambridge, U.K., 2000.

of **3** shows the loss of solvent molecules until 120 °C, followed by the loss of a bpdo molecule and one sulfur dioxide molecule, and finally decomposition starting at 270 °C. The XRPD studies on compounds **2** and **3** demonstrated that these compounds lose the solvent molecules very rapidly when exposed to air. This was accompanied by a drastic decrease of crystallinity and a change in the diffraction pattern. A following immersion in ethanol or other solvents such as water, methanol, or ethylene glycol confirmed the irreversible collapse of the porous structures of **2** and **3**; hence, they are not suitable for adsorption experiments. Compounds **4** and **5** are stable under atmospheric conditions. The measured XRPD patterns agree with the calculated patterns from the single-crystal analyses. Thermal analyses of **4** and **5** showed the loss of water molecules in two steps until 160 °C. In a first step until ca. 110 °C, the crystallized water molecules were lost; in a second step until 160 °C, the coordinated water molecules were lost. Final decomposition of **4** and **5** was found to begin at 290 °C.

Conclusions

Compounds **1**−**5** illustrate the diversity of structures that can be obtained by using bpdo as a ligand. It is shown that the choice of the anion is essential in network building. In structures **1**−**3**, the dithionate anions have a template effect and participate in the stabilization of the complete architecture through the formation of H bonds to the framework structure. The solvents used in the reactions also have an important influence. While the use of ethanolic solutions results in the formation of unique 2D (**1**) and 3D (**2** and **3**) structures, containing the stabilized dithionate anion, the reaction in water results in the decomposition of dithionate anions to sulfate anions, giving the stable mononuclear complexes **4** and **5**. The M−O−O−M torsion angles observed in **1**−**3** are similar to those observed previously (Figure 1S in the Supporting Information). The trans coordination mode of bpdo is favored, and a M−O−O−M torsion angle of 180° was found in compounds **1**−**3**. Additionally, the cis form was present in **2** and **3**, being essential to build up the 3D network. A M−O−O−M torsion angle of 44.8(2)° was observed and is in agreement with observations made on similar systems. A CCSD[10] search indicated that the M−O−N angles in bpdo complexes range from 105 to 150°, with a maximum at 125° (Figure 2S in the Supporting Information). Similar values were observed for the polymeric complexes **1**−**3**, with angles ranging from 119.0(1)° to 127.1(2)°. In contrast, in complexes where bpdo coordinates in a monodentate fashion, even larger M−O−N angles have been observed. This situation was also observed in complexes **4** and **5**, with angles of 132.3(2)° and 131.4(2)°, respectively. The aim of this study was to create new types of polymeric compounds, especially 3D frameworks, with reasonably high porosity for the study of their adsorption properties. The potential porosity of **2** and **3** is very high, up to ca. 50%, but unfortunately the removal of the guest molecules from the host results in the collapse of the 3D structure. Efforts are now being directed toward the synthesis of more stable framework compounds suitable for reversible guest adsorption. Nevertheless, new exciting multidimensional structures have been obtained showing the interplay of coordinating bonds and noncovalent interactions, such as H bonds and $\pi-\pi$-stacking interactions, between neutral and/or cationic and anionic charged parts, to build up these fascinating architectures.

Acknowledgment. We are grateful to Prof. K. V. Domasevitch, Inorganic Chemistry Department, Kiev University, Kiev, Ukraine, for supplying us with various metal dithionates. This work was supported by the Swiss National Science Foundation (Project Nos. FN 20-66642.01 and FN 20-103462.01 to H.S.-E.).

Supporting Information Available: Figures 1S and 2S, Table 1S, details of the crystallographic analyses, and X-ray crystallographic files (CIF) for compounds **1**−**5**. This material is available free of charge via the Internet at http://pubs.acs.org.

IC051934X